27. Dark Matter

Revised September 2017 by M. Drees (Bonn University) and G. Gerbier (Queen's University, Canada).

27.1. Theory

27.1.1. *Evidence for Dark Matter* :

The existence of Dark (*i.e.*, non-luminous and non-absorbing) Matter (DM) is by now well established [1,2]. The earliest, and perhaps still most convincing, evidence for DM came from the observation that various luminous objects (stars, gas clouds, globular clusters, or entire galaxies) move faster than one would expect if they only felt the gravitational attraction of other visible objects. An important example is the measurement of galactic rotation curves. The rotational velocity v of an object on a stable Keplerian orbit with radius r around a galaxy scales like $v(r) \propto \sqrt{M(r)/r}$, where $M(r)$ is the mass inside the orbit. If r lies outside the visible part of the galaxy and mass tracks light, one would expect $v(r) \propto 1/\sqrt{r}$. Instead, in most galaxies one finds that v becomes approximately constant out to the largest values of r where the rotation curve can be measured; in our own galaxy, $v \simeq 240$ km/s at the location of our solar system, with little change out to the largest observable radius. This implies the existence of a *dark halo*, with mass density $\rho(r) \propto 1/r^2$, *i.e.*, $M(r) \propto r$; at some point ρ will have to fall off faster (in order to keep the total mass of the galaxy finite), but we do not know at what radius this will happen. This leads to a lower bound on the DM mass density, $\Omega_{\rm DM} \gtrsim 0.1$, where $\Omega_X \equiv \rho_X/\rho_{\rm crit}$, $\rho_{\rm crit}$ being the critical mass density (*i.e.*, $\Omega_{\rm tot} = 1$ corresponds to a flat Universe).

The observation of clusters of galaxies tends to give somewhat larger values, $\Omega_{\rm DM} \simeq 0.2$. These observations include measurements of the peculiar velocities of galaxies in the cluster, which are a measure of their potential energy if the cluster is virialized; measurements of the *X-ray* temperature of hot gas in the cluster, which again correlates with the gravitational potential felt by the gas; and—most directly—studies of (weak) gravitational lensing of background galaxies on the cluster.

A particularly compelling example involves the bullet cluster (1E0657-558) which recently (on cosmological time scales) passed through another cluster. As a result, the hot gas forming most of the clusters' baryonic mass was shocked and decelerated, whereas the galaxies in the clusters proceeded on ballistic trajectories. Gravitational lensing shows that most of the total mass also moved ballistically, indicating that DM self-interactions are indeed weak [1].

Many cosmologists consider the existence of old galaxies (detected at redshift $z \sim 10$) to be the strongest argument for the existence of DM. Observations of the cosmic microwave background (CMB) show that density perturbations at $z \simeq 1,300$ were very small, $\delta\rho/\rho < 10^{-4}$. Since (sub–horizon sized) density perturbations grow only in the matter–dominated epoch, and matter domination starts earlier in the presence of DM, density perturbations start to grow earlier when DM is present, therefore allowing an earlier formation of the first galaxies [3].

All these arguments rely on Einsteinian, or Newtonian, gravity. One might thus ask whether the necessity to postulate the existence of DM, sometimes perceived to be ad hoc, could be avoided by modifying the theory of gravity. Indeed, the so–called Modified Newtonian Dynamics (MOND) allows to reproduce many observations on galactic scales, in particular galactic rotation curves, without introducing DM [4]. However, MOND is a purely non–relativistic theory. Attempts to embed it into a relativistic field theory require the existence of additional fields (e.g. a vector field or a second metric), and introduce considerably arbitrariness [4]. Moreover, the correct description of large–scale structure formation seems to require some sort of DM even in these theories [5]. In contrast, successful models of particle DM (see below) can be described in the well established language of quantum field theory, and do not need any modification of General Relativity, which has passed a large number of tests with flying colors [6].

The currently most accurate, if somewhat indirect, determination of $\Omega_{\rm DM}$ comes from global fits of cosmological parameters to a variety of observations; see the Section on Cosmological Parameters for details. For example, using measurements of the anisotropy of the cosmic microwave background (CMB) and of the spatial distribution of galaxies, Ref. 7 finds a density of cold, non-baryonic matter

$$\Omega_{\rm nbm} h^2 = 0.1186 \pm 0.0020 \ , \tag{27.1}$$

where h is the Hubble constant in units of 100 km/(s·Mpc). Some part of the baryonic matter density [7],

$$\Omega_{\rm b} h^2 = 0.02226 \pm 0.00023 \ , \tag{27.2}$$

may well contribute to (baryonic) DM, *e.g.*, MACHOs [8] or cold molecular gas clouds [9].

The DM density in the "neighborhood" of our solar system is also of considerable interest. This was first estimated as early as 1922 by J.H. Jeans, who analyzed the motion of nearby stars transverse to the galactic plane [2]. He concluded that in our galactic neighborhood, the average density of DM must be roughly equal to that of luminous matter (stars, gas, dust). Remarkably enough, a recent estimate finds a quite similar result for the smooth component of the local Dark Matter density [10]:

$$\rho_{\rm DM}^{\rm local} = (0.39 \pm 0.03) \cdot (1.2 \pm 0.2) \cdot (1 \pm \delta_{\rm triax}) \, \frac{\rm GeV}{\rm cm^3} \ . \tag{27.3}$$

The first term on the right-hand side of Eq. (27.3) gives the average Dark Matter density at a point one solar distance from the center of our galaxy. The second factor accounts for the fact that the baryons in the galactic disk, in which the solar system is located, also increase the local DM density [11]. The third factor in Eq. (27.3) corrects for possible deviations from a purely spherical halo; according to [12], $\delta_{\rm triax} \leq 0.2$. Small substructures (minihaloes, streams) are not likely to change the local DM density significantly [1]. Note that the first factor in Eq. (27.3) has been derived by fitting a complete model of our galaxy to a host of data, including the galactic rotation curve. A "purely local" analysis, only using the motion of nearby stars, gives a consistent result, with an error three times as large [13].

27.1.2. ***Candidates for Dark Matter*** :

Analyses of structure formation in the Universe indicate that most DM should be "cold" or "cool", *i.e.*, should have been non-relativistic at the onset of galaxy formation (when there was a galactic mass inside the causal horizon) [1]. This agrees well with the upper bound [7] on the contribution of light neutrinos to Eq. (27.1),

$$\Omega_\nu h^2 \leq 0.0062 \quad 95\% \text{ CL} . \tag{27.4}$$

Candidates for non-baryonic DM in Eq. (27.1) must satisfy several conditions: they must be stable on cosmological time scales (otherwise they would have decayed by now), they must interact very weakly with electromagnetic radiation (otherwise they wouldn't qualify as *dark* matter), and they must have the right relic density. Candidates include primordial black holes, axions, sterile neutrinos, and weakly interacting massive particles (WIMPs).

Primordial black holes (PBHs) must have formed before the era of Big-Bang nucleosynthesis, since otherwise they would have been counted in Eq. (27.2) rather than Eq. (27.1). Such an early creation of a large number of black holes is possible only in certain somewhat contrived cosmological models [14]. Moreover, a large number of astrophysical observations constrain PBH DM, leaving at best a narrow range of masses [15].

The existence of axions [16] was first postulated to solve the strong *CP* problem of QCD; they also occur naturally in superstring theories. They are pseudo Nambu-Goldstone bosons associated with the (mostly) spontaneous breaking of a new global "Peccei-Quinn" (PQ) U(1) symmetry at scale f_a; see the Section on Axions in this *Review* for further details. Although very light, axions would constitute cold DM, since they were produced non-thermally. At temperatures well above the QCD phase transition, the axion is massless, and the axion field can take any value, parameterized by the "misalignment angle" θ_i. At $T \lesssim 1$ GeV, the axion develops a mass $m_a \sim f_\pi m_\pi / f_a$ due to instanton effects. Unless the axion field happens to find itself at the minimum of its potential ($\theta_i = 0$), it will begin to oscillate once m_a becomes comparable to the Hubble parameter H. These coherent oscillations transform the energy originally stored in the axion field into physical axion quanta. The contribution of this mechanism to the present axion relic density is [1]

$$\Omega_a h^2 = \kappa_a \left(f_a / 10^{12} \text{ GeV} \right)^{1.175} \theta_i^2 , \tag{27.5}$$

where the numerical factor κ_a lies roughly between 0.5 and a few. If $\theta_i \sim \mathcal{O}(1)$, Eq. (27.5) will saturate Eq. (27.1) for $f_a \sim 10^{11}$ GeV, comfortably above laboratory and astrophysical constraints [16]; this would correspond to an axion mass around 0.1 meV. However, if the post-inflationary reheat temperature $T_R > f_a$, cosmic strings will form during the PQ phase transition at $T \simeq f_a$. Their decay will give an additional contribution to Ω_a, which is often bigger than that in Eq. (27.5) [1], leading to a smaller preferred value of f_a, *i.e.*, larger m_a. On the other hand, values of f_a near the Planck scale become possible if θ_i is for some reason very small.

"Sterile" $SU(2) \times U(1)_Y$ singlet neutrinos with keV masses [17] could alleviate the "cusp/core problem" [1] of cold DM models. If they were produced non-thermally through mixing with standard neutrinos, they would eventually decay into a standard neutrino and a photon or into three neutrinos.

Weakly interacting massive particles (WIMPs) χ are particles with mass roughly between 10 GeV and a few TeV, and with cross sections of approximately weak strength. Within standard cosmology, their present relic density can be calculated reliably if the WIMPs were in thermal and chemical equilibrium with the hot "soup" of Standard Model (SM) particles after inflation. In this case, their density would become exponentially (Boltzmann) suppressed at $T < m_\chi$. The WIMPs therefore drop out of thermal equilibrium ("freeze out") once the rate of reactions that change SM particles into WIMPs or vice versa, which is proportional to the product of the WIMP number density and the WIMP pair annihilation cross section into SM particles σ_A times velocity, becomes smaller than the Hubble expansion rate of the Universe. After freeze out, the co-moving WIMP density remains essentially constant; if the Universe evolved adiabatically after WIMP decoupling, this implies a constant WIMP number to entropy density ratio. Their present relic density is then approximately given by (ignoring logarithmic corrections) [3]

$$\Omega_\chi h^2 \simeq const. \cdot \frac{T_0^3}{M_{\rm Pl}^3 \langle \sigma_A v \rangle} \simeq \frac{0.1 \text{ pb} \cdot c}{\langle \sigma_A v \rangle} \ . \tag{27.6}$$

Here T_0 is the current CMB temperature, $M_{\rm Pl}$ is the Planck mass, c is the speed of light, σ_A is the total annihilation cross section of a pair of WIMPs into SM particles, v is the relative velocity between the two WIMPs in their cms system, and $\langle \ldots \rangle$ denotes thermal averaging. Freeze out happens at temperature $T_F \simeq m_\chi/20$ almost independently of the properties of the WIMP. This means that WIMPs are already non-relativistic when they decouple from the thermal plasma; it also implies that Eq. (27.6) is applicable if $T_R > T_F$. Notice that the 0.1 pb in Eq. (27.6) contains factors of T_0 and $M_{\rm Pl}$; it is, therefore, quite intriguing that it "happens" to come out near the typical size of weak interaction cross sections.

The seemingly most obvious WIMP candidate is a heavy neutrino. However, an SU(2) doublet neutrino will have too small a relic density if its mass exceeds $M_Z/2$, as required by LEP data. One can suppress the annihilation cross section, and hence increase the relic density, by postulating mixing between a heavy SU(2) doublet and some sterile neutrino. However, one also has to require the neutrino to be stable; it is not obvious why a massive neutrino should not be allowed to decay.

The currently best motivated WIMP candidate is, therefore, the lightest superparticle (LSP) in supersymmetric models [18] with exact R-parity (which guarantees the stability of the LSP). Searches for exotic isotopes [19] imply that a stable LSP has to be neutral. This leaves basically two candidates among the superpartners of ordinary particles, a sneutrino, and a neutralino. The negative outcome of various WIMP searches (see below) rules out "ordinary" sneutrinos as primary component of the DM halo of our galaxy. The most widely studied WIMP is therefore the lightest neutralino. Detailed calculations [1] show that the lightest neutralino will have the desired thermal relic density Eq. (27.1) in

at least four distinct regions of parameter space. χ could be (mostly) a bino or photino (the superpartner of the $U(1)_Y$ gauge boson and photon, respectively), if both χ and some sleptons have mass below ~ 150 GeV, or if m_χ is close to the mass of some sfermion (so that its relic density is reduced through co-annihilation with this sfermion), or if $2m_\chi$ is close to the mass of the *CP*-odd Higgs boson present in supersymmetric models. Finally, Eq. (27.1) can also be satisfied if χ has a large higgsino or wino component.

Many non-supersymmetric extensions of the Standard Model also contain viable WIMP candidates [1]. Examples are the lightest $T-$odd particle in "Little Higgs" models with conserved $T-$parity, or "techni-baryons" in scenarios with an additional, strongly interacting ("technicolor" or similar) gauge group.

Although thermally produced WIMPs are attractive DM candidates because their relic density naturally has at least the right order of magnitude, non-thermal production mechanisms have also been suggested, *e.g.*, LSP production from the decay of some moduli fields [20], from the decay of the inflaton [21], or from the decay of "$Q-$balls" (non-topological solitons) formed in the wake of Affleck-Dine baryogenesis [22]. Although LSPs from these sources are typically highly relativistic when produced, they quickly achieve kinetic (but not chemical) equilibrium if T_R exceeds a few MeV [23] (but stays below $m_\chi/20$). They therefore also contribute to cold DM. Finally, if the WIMPs aren't their own antiparticles, an asymmetry between WIMPs and antiWIMPs might have been created in the early Universe, possibly by the same (unknown) mechanism that created the baryon antibaryon asymmetry. In such "asymmetric DM" models [24] the WIMP antiWIMP annihilation cross section $\langle \sigma_A v \rangle$ should be significantly larger than $0.1\,\mathrm{pb}\cdot c$, cf Eq. (27.6).

The absence of signals at the LHC for physics beyond the Standard Model, as well as the discovery of an SM-like Higgs boson with mass near 125 GeV, constrains many well-motivated WIMP models. For example, in constrained versions of the minimal supersymmetrized Standard Model (MSSM) both the absence of supersymmetric signals and the relatively large mass of the Higgs boson favor larger WIMP masses and lower scattering cross sections on nucleons. However, constraints from "new physics" searches apply most directly to strongly interacting particles. Many WIMP models therefore can still accommodate a viable WIMP for a wide range of masses. For example, in supersymmetric models where the bino mass is not related to the other gaugino masses a bino with mass as small as 15 GeV can still have the correct thermal relic density [25]. Even lighter supersymmetric WIMPs can be realized in models with extended Higgs sector [26].

The lack of signals at the LHC may have weakened the argument for WIMPs being embedded in a larger theory that addresses the hierarchy problem. This, and the increasingly stronger limits from direct and indirect WIMP searches (see below), has spawned a plethora of new models of particle DM. For example, particles with masses in the MeV to GeV range still naturally form cold DM, but are difficult to detect with current methods. These models typically require rather light "mediator" particles in order to achieve the correct thermal relic density. Light bosons coupling to (possibly quite heavy) DM particles have also been invoked in order to greatly increase the annihilation cross section of the latter at small velocities, through the

so-called Sommerfeld enhancement [27]. Several collider and fixed target experiments have searched for such light mediators, but no signal has been found [28].

Another mechanism to achieve the correct thermal relic density is based on $2 \leftrightarrow 3$ reactions purely within the dark sector. This requires quite large self interactions between the DM particles, which have therefore been dubbed SIMPs (strongly interacting massive particles) [29]. The SIMP-SIMP elastic scattering cross section σ might even be large enough to affect cosmological structure formation, which roughly requires $\sigma/m_\chi > 0.1$ b/GeV, where m_χ is the mass of the SIMP; this is considerably larger than the elastic scattering cross section of protons. Scalar SIMPs could interact with ordinary matter via Higgs exchange.

Primary black holes (as MACHOs), axions, sterile neutrinos, and WIMPs are all (in principle) detectable with present or near-future technology (see below). There are also particle physics DM candidates which currently seem almost impossible to detect, unless they decay; the present lower limit on their lifetime is of order 10^{25} to 10^{26} s for 100 GeV particles. These include the gravitino (the spin-3/2 superpartner of the graviton), states from the "hidden sector" thought responsible for supersymmetry breaking, and the axino (the spin-1/2 superpartner of the axion) [1].

27.2. Experimental detection of Dark Matter

27.2.1. *The case of baryonic matter in our galaxy* :

The search for hidden galactic baryonic matter in the form of MAssive Compact Halo Objects (MACHOs) has been initiated following the suggestion that they may represent a large part of the galactic DM and could be detected through the microlensing effect [8]. The MACHO, EROS, and OGLE collaborations have performed a program of observation of such objects by monitoring the luminosity of millions of stars in the Large and Small Magellanic Clouds for several years. EROS concluded that MACHOs cannot contribute more than 8% to the mass of the galactic halo [30], while MACHO observed a signal at 0.4 solar mass and put an upper limit of 40%. Overall, this strengthens the need for non-baryonic DM, also supported by the arguments developed above.

27.2.2. *Axion searches* :

Axions can be detected by looking for $a \to \gamma$ conversion in a strong magnetic field [1]. Such a conversion proceeds through the loop-induced $a\gamma\gamma$ coupling, whose strength $g_{a\gamma\gamma}$ is an important parameter of axion models. There is currently only one experiment searching for axionic DM: the ADMX experiment [31], originally situated at the LLNL in California but now running at the University of Washington, started taking data in the first half of 1996. It employs a high quality cavity, whose "Q factor" enhances the conversion rate on resonance, *i.e.*, for $m_a(c^2 + v_a^2/2) = \hbar\omega_{\rm res}$. One then needs to scan the resonance frequency in order to cover a significant range in m_a or, equivalently, f_a. ADMX now uses SQUIDs as first-stage amplifiers; their extremely low noise temperature (1.2 K) enhances the conversion signal. Published results [32], combining data taken with conventional amplifiers and SQUIDs, exclude axions with mass between 1.9 and 3.53 μeV, corresponding to $f_a \simeq 4 \cdot 10^{13}$ GeV, for an assumed local DM density of 0.45

GeV/cm^3, if $g_{a\gamma\gamma}$ is near the upper end of the theoretically expected range. About five times better limits on $g_{a\gamma\gamma}$ were achieved [33] for 1.98 μeV $\leq m_a \leq$ 2.18 μeV as well as for 3.3 μeV $\leq m_a \leq$ 3.65 μeV, if a large fraction of the local DM density is due to a single flow of axions with very low velocity dispersion. The ADMX experiment is being upgraded by reducing the cavity and SQUID temperature from the current 1.2 K to about 0.1 K. This should increase the frequency scanning speed for given sensitivity by more than two orders of magnitude, or increase the sensitivity for fixed observation time.

Recently several new DM axion search experiments have been proposed and are in various stages of development; see ref. [34] for brief descriptions and further references. However, none of them has produced any limits yet.

27.2.3. *Searches for keV Neutrinos* :

Relic keV neutrinos ν_s can only be detected if they mix with the ordinary neutrinos. This mixing leads to radiative $\nu_s \to \nu\gamma$ decays, with lifetime $\tau_{\nu_s} \simeq 1.8 \cdot 10^{21}\ \mathrm{s} \cdot (\sin\theta)^{-2} \cdot (1\ \mathrm{keV}/m_{\nu_s})^5$, where θ is the mixing angle [17]. This gives rise to a flux of mono-energetic photons with $E_\gamma = m_{\nu_s}/2$, which might be observable by *X-ray* satellites. In the simplest case the relic ν_s are produced only by oscillations of standard neutrinos. Assuming that all lepton-antilepton asymmetries are well below 10^{-3}, the ν_s relic density can then be computed uniquely in terms of the mixing angle θ and the mass m_{ν_s}. The combination of lower bounds on m_{ν_s} from analyses of structure formation (in particular, the Lyα "forest") and upper bounds on *X-ray* fluxes from various (clusters of) galaxies exclude this scenario if ν_s forms all of DM. This conclusion can be evaded if ν_s forms only part of DM, and/or if there is a lepton asymmetry $\geq 10^{-3}$ (i.e. some 7 orders of magnitude above the observed baryon-antibaryon asymmetry), and/or if there is an additional source of ν_s production in the early Universe, e.g. from the decay of heavier particles [17].

Recently some evidence for a weak *X-ray* line at $\sim$ 3.5 keV has been found in data released by the XMM-Newton satellite [35]. However, the existence of this line was not confirmed by data from the Suzaku and (very short-lived) Hitomi missions [36]. Although this line has been interpreted in terms of decaying keV DM particles, e.g. sterile neutrinos with mass $m_{\nu_s} \simeq 7$ keV, it might also be due to certain inner-shell transitions of highly ionized K atoms [37].

27.2.4. *Basics of direct WIMP search* :

As stated above, WIMPs should be gravitationally trapped inside galaxies and should have the adequate density profile to account for the observed rotational curves. These two constraints determine the main features of experimental detection of WIMPs, which have been detailed in the reviews in [1].

Their mean velocity inside our galaxy relative to its center is expected to be similar to that of stars, *i.e.*, a few hundred kilometers per second at the location of our solar system. For these velocities, WIMPs interact with ordinary matter through elastic scattering on nuclei. With expected WIMP masses in the range 10 GeV to 10 TeV, typical nuclear recoil energies are of order of 1 to 100 keV.

The shape of the nuclear recoil spectrum results from a convolution of the WIMP velocity distribution, usually taken as a Maxwellian distribution in the galactic rest frame, shifted into the Earth rest frame, with the angular scattering distribution, which is isotropic to first approximation but forward-peaked for high nuclear mass (typically higher than Ge mass) due to the nuclear form factor. Overall, this results in a roughly exponential spectrum. The higher the WIMP mass, the higher the mean value of the exponential. This points to the need for low nuclear recoil energy threshold detectors.

On the other hand, expected interaction rates depend on the product of the local WIMP flux and the interaction cross section. The first term is fixed by the local density of dark matter, taken as 0.39 GeV/cm^3 [see Eq. (27.3)], the mean WIMP velocity, typically 220 km/s, the galactic escape velocity, typically 544 km/s [38] and the mass of the WIMP. The expected interaction rate then mainly depends on two unknowns, the mass and cross section of the WIMP (with some uncertainty [10] due to the halo model). This is why the experimental observable, which is basically the scattering rate as a function of energy, is usually expressed as a contour in the WIMP mass–cross section plane.

The cross section depends on the nature of the couplings. For non-relativistic WIMPs, one in general has to distinguish spin-independent and spin-dependent couplings. The former can involve scalar and vector WIMP and nucleon currents (vector currents are absent for Majorana WIMPs, *e.g.*, the neutralino), while the latter involve axial vector currents (and obviously only exist if χ carries spin). Due to coherence effects, the spin-independent cross section scales approximately as the square of the mass of the nucleus, so higher mass nuclei, from Ge to Xe, are preferred for this search. For spin-dependent coupling, the cross section depends on the nuclear spin factor; used target nuclei include ^{19}F, ^{23}Na, ^{73}Ge, ^{127}I, ^{129}Xe, ^{131}Xe, and ^{133}Cs.

Cross sections calculated in MSSM models [39] induce rates of at most 1 evt day^{-1} kg^{-1} of detector, much lower than the usual radioactive backgrounds. This indicates the need for underground laboratories to protect against cosmic ray induced backgrounds, and for the selection of extremely radio-pure materials.

The typical shape of exclusion contours can be anticipated from this discussion: at low WIMP mass, the sensitivity drops because of the detector energy threshold, whereas at high masses, the sensitivity also decreases because, for a fixed mass density, the WIMP flux decreases $\propto 1/m_\chi$. The sensitivity is best for WIMP masses near the mass of the recoiling nucleus.

Two important points are to be kept in mind when comparing exclusion curves from various experiments between them or with positive indications of a signal.

For an experiment with a fixed nuclear recoil energy threshold, the lower is the considered WIMP mass, the lower is the fraction of the spectrum to which the experiment is sensitive. This fraction may be extremely small in some cases. For illustration, some figures from some early experiments are used in the following. CoGeNT [40], using a Germanium detector with an energy threshold of around 2 keV, is sensitive to about 10 % of the total recoil spectrum of a 7 GeV WIMP, while for XENON100 [41], using a liquid Xenon detector with a threshold of 8.4 keV, this fraction is only 0.05 % (that is the extreme tail of the distribution), for the same WIMP mass. The two experiments are

then sensitive to very different parts of the WIMP velocity distribution.

A second important point to consider is the energy resolution of the detector. Again at low WIMP mass, the expected roughly exponential spectrum is very steep and when the characteristic energy of the exponential becomes of the same order as the energy resolution, the energy smearing becomes important. In particular, a significant fraction of the expected spectrum below effective threshold is smeared above threshold, increasing artificially the sensitivity. For instance, a Xenon detector with a threshold of 8 keV and infinitely good resolution is actually insensitive to a 7 GeV mass WIMP, because the expected energy distribution has a cut-off at roughly 5 keV. When folding in the experimental resolution of XENON100 (corresponding to a photostatistics of 0.5 photoelectron per keV), then around 1 % of the signal is smeared above 5 keV and 0.05 % above 8 keV. Setting reliable cross section limits in this mass range thus requires a complete understanding of the response of the detector at energies well below the nominal threshold.

Two experimental signatures are predicted for WIMP signals. One is a strong daily forward/backward asymmetry of the nuclear recoil direction, due to the alternate sweeping of the WIMP cloud by the rotating Earth. Detection of this effect requires gaseous detectors, anisotropic response scintillators (stilbene) or extremely fine grain solid state detector (emulsion). The second is a few percent annual modulation of the recoil rate due to the Earth speed adding to or subtracting from the speed of the Sun. This tiny effect can only be detected with large masses; nuclear recoil identification should also be performed, as the otherwise much larger background may also be subject to seasonal modulation.

27.2.5. *Status and prospects of direct WIMP searches* :

Given the intense activity of the field, readers interested in more details than the ones given below may refer to [1], to presentations at recent conferences [31] and to the previous versions of this review.

The first searches have been performed with ultra-pure semiconductors installed in pure lead and copper shields in underground environments. Combining a priori excellent energy resolutions and very pure detector material, they produced the first limits on WIMP searches (Heidelberg-Moscow, IGEX, COSME-II, HDMS) [1]. Planned experiments using several tens of kg to a ton of Germanium run at liquid nitrogen temperature (designed for double-beta decay search) – GERDA, MAJORANA – are based in addition on passive reduction of the external and internal electromagnetic and neutron background by using Point Contact detectors (discussed below), minimal detector housing, close electronics, pulse shape discrimination and large liquid nitrogen or argon shields. Their sensitivity to WIMP interactions will depend on their ability to lower the energy threshold sufficiently, while keeping the background rate small.

Development of so called Point Contact Germanium detectors, with a very small capacitance allowed one to reach sub-keV thresholds, though performance seems to stall now at around 400 eV. The CoGeNT collaboration was first operating a single 440 g Germanium detector with an effective threshold of 400 eV in the Soudan Underground Laboratory for 56 days [40]. No new result has been published these last two years. A

possible excess that had originally been observed has been understood, while a possible annual modulation in the data fell short of being significant as well.

The CDEX collaboration has also operated a single Point Contact detector in the Jinping underground laboratory, with a 475 eV threshold and a background rate too high to lead to a competitive limit [42]. The next step is CDEX-10, an array with a total mass of 10 kg, planned to be immersed in a ton-scale liquid argon chamber as active shield.

In order to make progress in the reliability of any claimed signal, active background rejection and signal identification questions have to be addressed. Active background rejection in detectors relies on the relatively small ionization in nuclear recoils due to their low velocity. This induces a reduction ("quenching") of the ionization/scintillation signal for nuclear recoil signal events relative to e or γ induced backgrounds of the same energy. Energies calibrated with gamma sources are then called "electron equivalent energies" (keVee unit used below). This effect has been both calculated and measured [1]. It is exploited in cryogenic detectors described later. In scintillation detectors, it induces in addition a difference in decay times of pulses induced by e/γ events vs nuclear recoils. In most cases, due to the limited resolution and discrimination power of this technique at low energies, this effect allows only a statistical background rejection. It has been used in NaI(Tl) (DAMA, LIBRA, NAIAD, Saclay NaI), in CsI(Tl) (KIMS), and Xe (ZEPLIN-I) [1,31]. In liquid argon, pulse shape discrimination applied to the pulse of primary scintillation light is particularly efficient and allows an event by event discrimination, however, at some high energy, roughly above 20 keVee (see later in this review).

The DAMA collaboration is the only group in the community claiming a signal at more than 5 σ level, observed now for 14 years. The claim results from a total of 7 years exposure with the LIBRA phase involving 250 kg of detectors, plus the earlier 6 years exposure of the original DAMA/NaI experiment with 100 kg of detectors [43], for a total exposure of 1.33 t·y. They observe an annual modulation of the signal in the 2 to 6 keVee bin, with the expected period (1 year) and phase (maximum around June 2), at 9.3 σ level. If interpreted within the standard halo model described above, two possible solutions have been proposed: a WIMP with $m \simeq 50$ GeV and $\sigma_{\chi p} \simeq 7 \cdot 10^{-6}$ pb (central values) or at low mass, in the 6 to 16 GeV range with $\sigma_{\chi p} \simeq 2 \cdot 10^{-4}$ pb; the cross section could be somewhat lower if there is a significant channeling effect [1]. No new result has been reported by DAMA over the two last years.

Interpreting these observations as positive WIMP signal raises several issues of internal consistency. First, the proposed WIMP solutions would induce a sizable fraction of nuclear recoils in the total measured rate in the 2 to 6 keVee bin. No pulse shape analysis has been reported by the authors to check whether the unmodulated signal was detectable this way. Secondly, the residual e/γ-induced background, inferred by subtracting the signal predicted by the WIMP interpretation from the data, has an unexpected shape [44], starting near zero at threshold and quickly rising to reach its maximum near 3 to 3.5 keVee; from general arguments one would expect the background (e.g. due to electronic noise) to increase towards the threshold. Finally, the amplitude of the annual modulation shows a tendency to decrease with time [45].

Under standard assumptions, many experiments – see below – exclude both the high and low mass DAMA/LIBRA solutions by increasingly many orders of magnitude. In particular, the large WIMP mass (60 GeV) interpretation of the DAMA/LIBRA signal induced by scattering on Iodine nuclei is excluded directly by the Korean collaboration KIMS. It has conducted an experiment in the underground Yangyang laboratory in South Korea using CsI(Tl), *i.e.* the identical nucleus of Iodine, and set an upper limit on the cross section roughly two orders of magnitude below that required to explain the DAMA signal [46]. On the other hand, no convincing non-WIMP explanation of the annual modulation of the DAMA/LIBRA signal has yet been put forward.

The last few years have seen a growing number of projects using NaI(Tl) scintillators (SABRE, COSINE; and DM-ICE, KIMS and ANAIS now taking data). Some of them have now reached the needed maturity to test the DAMA result. Thanks to the progress in powder selection and reduction of key contaminants, the background rate at low energy obtained by COSINE is only about a factor 2 higher than DAMA's. Moreover, they obtained a light yield two times higher than the ones previously achieved. This opens the possibility of a significant nuclear recoil-electron recoil discrimination at energies down to 2 keV [47]. The COSINE team is now operating 100 kg of detectors and prepares a second phase of 200 kg.

DM-ICE has published results [48] of a 3.6 y run with 18 kg operated within the Ice Cube neutrino Telescope, at a threshold of 4 keV. Not surprisingly, no modulation was observed.

SABRE plans to run NaI(Tl) detectors immersed in liquid scintillatior in two similar set-ups at LNGS and in the Southern hemisphere, in the new underground laboratory site STAWELL in Australia (in a gold mine 240 km west of Melbourne) in order to test for a possible shift of the phase of the annual modulation. Such a shift would be expected if the modulation is somehow related to the seasons on Earth, whereas a WIMP induced annual modulation should have the same phase in both hemispheres. SABRE has conducted an R&D program to improve the radiopurity of their crystals and light detectors and will soon start first proof of principle measurements at LNGS.

Liquid noble gas (Xe, Ar) detectors have achieved tremendous progress. Due to their relatively easy scalability they currently have the highest sensitivity for "high mass" WIMPs (masses above ~ 10 GeV). Dual (liquid and gas) phase detectors allow one to measure both the primary scintillation S1 and the ionization electrons drifted through the liquid, amplified in the gas and giving rise to a second scintillation pulse S2. S1 and S2 are used to discriminate between nuclear and electron recoils as well as 3D position reconstruction within the detector. In the single phase mode (DEAP, XMASS), only S1 is measured; discrimination is then ensured by the pulse shape analysis in the case of Argon and by the self shielding in the case of Xenon.

The suite of XENON-n detectors [31] are operated at the Gran Sasso laboratory. After XENON10, XENON 100 in 2012 was the first to clearly show the supremacy of liquid noble gas detectors for high mass WIMP searches. Recently the last avatar, Xenon1t, has delivered its first results [49]. With a fiducial mass of 1042 kg and 32 days of operating time, they set the best limit on the cross section for spin-independent interactions at 7.7×10^{-11} pb for a WIMP mass of 35 GeV.

This result surpasses the most recent limit set by LUX, a 370 kg double phase Xenon detector installed in a large water shield, operated in the SURF (previously Homestake) laboratory in the US. Thanks to a total exposure of 33500 kg·d, a limit is set at 1.1×10^{-10} pb for a WIMP mass of 50 GeV [50]. This data set provides the best published limit for spin dependent WIMPs with pure neutron couplings at all masses [51]. LUX is now preparing the next phase, LZ, which will operate several tons of Xenon.

PandaX, another double phase liquid Xenon based project, has been quickly evolving in the Chinese Jinping lab. From a first phase of 54 kg, the detector has been upgraded within about one year to a mass of 500 kg. The latest result was obtained by PandaX-II with a fiducial mass of 364 kg and a running time of 77 days [52]. Combined with previous data, the total exposure of 54 000 kg·d allows one to set a limit of 8.6×10^{-11} pb for a WIMP mass of 40 GeV [53]. There is now a strong competition between these three experiments.

XMASS [31], a single-phase 800 kg Xenon detector (100 kg fiducial mass, allowing a strong self shielding) operated in Japan at the SuperKamiokande site, has seen its detector repaired. The observed spectrum is consistent with the expected background and allows to set limits about 2 orders of magnitude higher than the other, double phase, detectors. The next phase of XMASS is XMASS-1.5 with a 1.5 ton fiducial mass.

The ArDM-1t detector [31], an Argon detector with a total mass of 1.1 t installed at the Canfranc laboratory, is still in the commissioning phase.

DarkSide50, installed in LNGS, is a two phase liquid argon TPC with fiducial mass of 46 kg. The detector is immersed in a spherical vessel containing 30 t of liquid scintillator, which in turn is immersed in a tank containing one kiloton of pure water. Results from the first use of Argon from underground sources, which is depleted in the radioactive isotope ^{39}Ar, have been published recently [54]. Combined with previous results obtained with natural Argon, the obtained limit is 2.0×10^{-8} pb for a WIMP mass of 100 GeV.

DEAP-3600 [31], designed to operate in single phase mode in spherical geometry, started operating at SNOLAB 3600 kg of Argon, the so far largest mass of liquid noble gas for dark matter search. A short data taking run of 4.2 days in August 2016 resulted in a sizable exposure of 9 870 kg·d in which no candidate event was observed in the region of interest, allowing to set a limit of 1.2×10^{-8} pb for a WIMP mass of 100 GeV [55]. This is currently the best limit for an Argon based detector. However, in the background free regime, even with a fiducial mass a factor 2 higher than Xenon1t, the rate of increase in sensitivity per unit time of DEAP is around a factor 6 lower than Xenon1t. This is due to the high threshold of DEAP and the lower enhancement factor for spin independent interactions on Argon compared to Xenon. The final "winner" will then be the one with the lowest ultimate background, which DEAP projects to be.

Candidates for the next generation of multiton Ar and Xe detectors are XENONnT, DARWIN, DEAP-50T, and DarkSide-20k.

At mK temperature, the simultaneous measurement of the phonon and ionization signals in semiconductor detectors permits event by event discrimination between nuclear and electronic recoils down to few keV recoil energy. This feature is being used by the CDMS [31] and EDELWEISS [31] collaborations. Surface interactions, exhibiting

incomplete charge collection, are an important residual background. Both experiments now use an interleaved ionization read-out electrodes scheme in order to control this background. On the other hand, the cryogenic experiment CRESST [31] in the Gran Sasso laboratory uses scintillating crystals as detectors and thus employs the scintillation signal as second variable for background discrimination.

Somewhat paradoxically, all three cryogenic experiments now tend to turn their efforts towards a mode of operating their detectors which gives up their discrimination power. Indeed, given the overwhelming progress of liquid noble gas detectors for WIMP masses above 10 GeV, cryogenic detectors are now tuned towards access to low mass WIMPs, by decreasing their thresholds. Given that the current limits on cross sections below a WIMP mass of 10 GeV are rather high, the detector mass required to get significant improvements does not need to be large, and discrimination against electron recoils is less crucial. Typically, in the present situation, the current limits on scattering cross sections of 3 GeV WIMPs are 5 orders of magnitude higher than at 30 GeV, which means that a detector mass of about 100 g is enough to gain in sensitivity at a WIMP mass of 3 GeV. In order to reach the "neutrino floor" due to the irreducible background rate from the elastic scattering of (mostly solar) neutrinos off the target nuclei [56] in the 7 GeV region, that is 10^{-8} pb for the WIMP–proton cross section, a detector mass of 50 to 200 kg would be needed.

The SuperCDMS collaboration has now stopped operations at Soudan and is preparing to install its large cryostat, able to house up to 200 kg of detectors, at SNOLAB. They reported recently the results from the majority of the Soudan data set, involving 15 Germanium IZIP detectors and an exposure of 1690 kg·d. A new spin-independent WIMP nucleon cross sections limit is set at 1.4×10^{-8} pb, at 90% CL for a 46 GeV WIMP [57]. This is a 20% improvement relative to the 2015 result involving 612 kg·d . Combining both results provides a limit of 1.0×10^{-8} pb at 90% CL for a 46 GeV WIMP. For comparison, the best limit at the same WIMP mass set by Xenon detectors is around 0.8×10^{-11} pb, *i.e.* two orders of magnitude lower.

Some detectors at Soudan have been operated with "high" voltage (*i.e.* 70 V instead of 6 to 8 V) across the electrodes measuring the ionization. The phonons generated by the ionization electrons traveling inside the crystal – the so-called Neganov Luke effect – then give a stronger phonon signal than the normal phonon pulse induced by the initial interaction. This is equivalent to an amplification of the ionization pulse, but at the expense of losing the discrimination between electron and nuclear recoils. This running mode allowed to lower the energy threshold to 50 to 70 eVee [58]. The sensitivity is then determined by the counting rate at the threshold. A significant improvement of the cross section limit, to 2.0×10^{-5} pb, has been obtained at around 3 GeV of WIMP mass. A projection paper [59] details expected performances for the SNOLAB set-up. A typical figure for the sensitivity goal is 4.0×10^{-8} pb for a 3 GeV WIMP. Calculated sensitivities down to a WIMP mass of 1 GeV rely on the extrapolation of knowledge of the radioactive background down to 10 eVee and of the quenching factor down to 50 eVNR.

The EDELWEISS collaboration [31] also operates cryogenic Germanium detectors (so-called FID800 detectors, featuring a complete coverage of the crystal with annular electrodes, and better rejection of non-nuclear recoil events) in the Laboratoire Souterrain

de Modane. Two new results based on the same data set have been published. From an exposure of 496 kg·d obtained with 8 detectors selected out of 24 detectors for their very low threshold [60], a profile likelihood analysis has been applied and provided limits ranging from 1.6×10^{-3} pb at around 4 GeV to 7.0×10^{-8} pb at 30 GeV, all limits being higher than the ones obtained by SuperCDMS in similar mass ranges. A strategy paper [61] details expected performances under various hypothesis of R&D outcomes and running conditions. An improvement of a factor 3 over the current SuperCDMS result is anticipated at a WIMP mass of 3 GeV in 2018. The route towards the detection of solar ^{8}B neutrinos, involving several hundred kg of discrimination detectors in the SNOLAB SuperCDMS set-up, assumes an improvement in ionization channel energy rms resolution of 50 eVee, which is considered to be at hand. The solar neutrinos would be detected by elastic (coherent) scattering off the Germanium nuclei; coherent neutrino–nucleus scattering has very recently been detected experimentally for the first time [62].

The cryogenic experiment CRESST [31] in the Gran Sasso laboratory uses the scintillation of $CaWO_4$ crystals as second variable for background discrimination. CRESST puts focus on lowering the energy threshold in order to access low mass WIMPs, by implementing a new generation of detectors with improved vetoing of low energy surface events induced by external alpha particles. Results [63] from a single detector show a quite low threshold of 0.31 keVNR, allowing one to set a limit on WIMP–proton cross section for spin independent couplings of 3×10^{-4} pb for a WIMP mass around 3 GeV and 10^{-2} pb at 1 GeV, assuming interactions on the Oxygen nuclei in the target. Interestingly, the obtained limit excludes the signals reported by the same collaboration two years before, which are now believed to have been caused by an inadequate description of the background from external alpha particles. Low mass 20 g detectors with thresholds of around 100 eV are now being operated. As illustration of the shift towards extremely low threshold, 1 g detectors with 20 eV threshold have been operated at the surface in order to set limits on MeV mass particles [64].

The two following experiments also aim to search for very low mass WIMPs, that is down to 0.1 GeV. DAMIC [31], using CCDs at SNOLAB, obtained a threshold of around 100 eV. Thanks to a series of exposures of 2.9 g CCDS in different conditions adding to 0.6 kg·d, an exclusion limit [65] has been produced, ranging from 1 pb at 1.5 GeV to 1×10^{-3} pb at 3 GeV, above the limits set by CRESST. The DAMIC100 project will use 16 CCDs of 5.8 g each. The renamed NEWS-G collaboration [31] exploits an unconventional gas detector, based on a spherical geometry, able to achieve a very low energy threshold, down to a single ionization electron. A 60 cm diameter prototype, SEDINE, has being operated in the Fréjus laboratory with Neon gas at a pressure of 3.1 bars for 42 days. With a 150 eV analysis threshold, a quite competitive limit [66] of 4.4×10^{-1} pb is set at a WIMP mass of 0.5 GeV. The NEWS-SNO project involving a 1.4 m diameter spherical detector has been accepted at SNOLAB, and will allow to reach sensitivity to WIMP masses down to 0.1 GeV thanks to the use of Helium and Hydrogen targets.

Detectors based on metastable liquids or gels have the advantage of being insensitive to electromagnetic interactions, and the drawback of being threshold yes/no detectors. PICO, the merging of the Picasso and COUPP collaborations, has operated at SNOLAB

a series of bubble chamber type detectors with compounds rich in Fluorine, therefore orienting their search towards spin dependent interactions. Spectacular progress has been achieved in the last two years thanks to the removal of particulates responsible for anomalous nuclear recoil like events. Using PICO60, filled with 54 kg of C_3F_8, no single scatter compatible with a nuclear recoil has been observed in an exposure of 1167 kg·d, allowing to set a limit on the spin dependent proton cross section of 3.4×10^{-5} pb for a 30 GeV WIMP, a gain of almost a factor 20 relative to the previous limit. This experiment has the best sensitivity worldwide for spin dependent couplings at all WIMP masses, similar to the ones derived from the bound on WIMP-induced muon neutrinos from the Sun (see below). The collaboration has submitted the PICO-500 project, a ton scale detector, which has been funded and will be operated at SNOLAB.

If a hint for a signal is observed in calorimetric detectors, the only convincing way to prove the galactic origin of a possible signal would be to show that the direction of nuclear recoils is indeed compatible with that of the expected WIMP wind on Earth. Until recently the low pressure Time Projection Chamber technique seemed the only feasible way to measure tracks [1]. The DRIFT collaboration [31] has operated a 1 m^3 volume detector filled with CS2 in the UK Boulby mine. Results from a 55 days run with a partial pressure of 10 torr of CF4 did not show any candidate event but the extracted limit of 0.28 pb at 100 GeV WIMP mass is 5 orders of magnitude higher than the limit set by PICO. The MIMAC collaboration [31], who operates an unshielded 2.5 l 1000 channel prototype in the Laboratoire Souterrain de Modane, did not conduct any WIMP search. Other groups developing similar techniques, though with lower sensitivity, are DMTPC in the US and NewAge in Japan. A newcomer in the WIMP directional measurement hunt, NEWSdm, an Italo-Japanese collaboration building on know-how acquired with the emulsion technique in the OPERA experiment, proposes to measure the expected 0.1 micron long nuclear tracks in an extremely finely grained emulsion. R&D is ongoing and proponents aim at operating a target mass of 1 kg, with a final sensitivity expected to be at around the DAMA signal, *i.e.* well above current limits set by most calorimetric experiments.

To complete this review about direct detection of dark matter, it is certainly worth mentioning a growing wave of ideas for new avenues towards detection of dark matter particles with ever lower masses, ranging from MeV down to the meV mass scale. Suggested methods include scattering on nuclei, scattering on electrons, absorption of bosonic particles by electrons, and chemical bond breaking. Since these proposals have the potential to explore new territories, small scale experiments can quickly cover orders of magnitude in mass and sensitivity of new parameter space.

Figures 27.1 and 27.2 illustrate the limits and positive claims for WIMP scattering cross sections, normalized to scattering on a single nucleon, for spin independent and spin dependent couplings, respectively, as functions of WIMP mass. Only the two or three currently best limits are presented. Also shown are constraints from indirect observations (see the next section) and a typical region of a SUSY model after the LHC run-1 results.

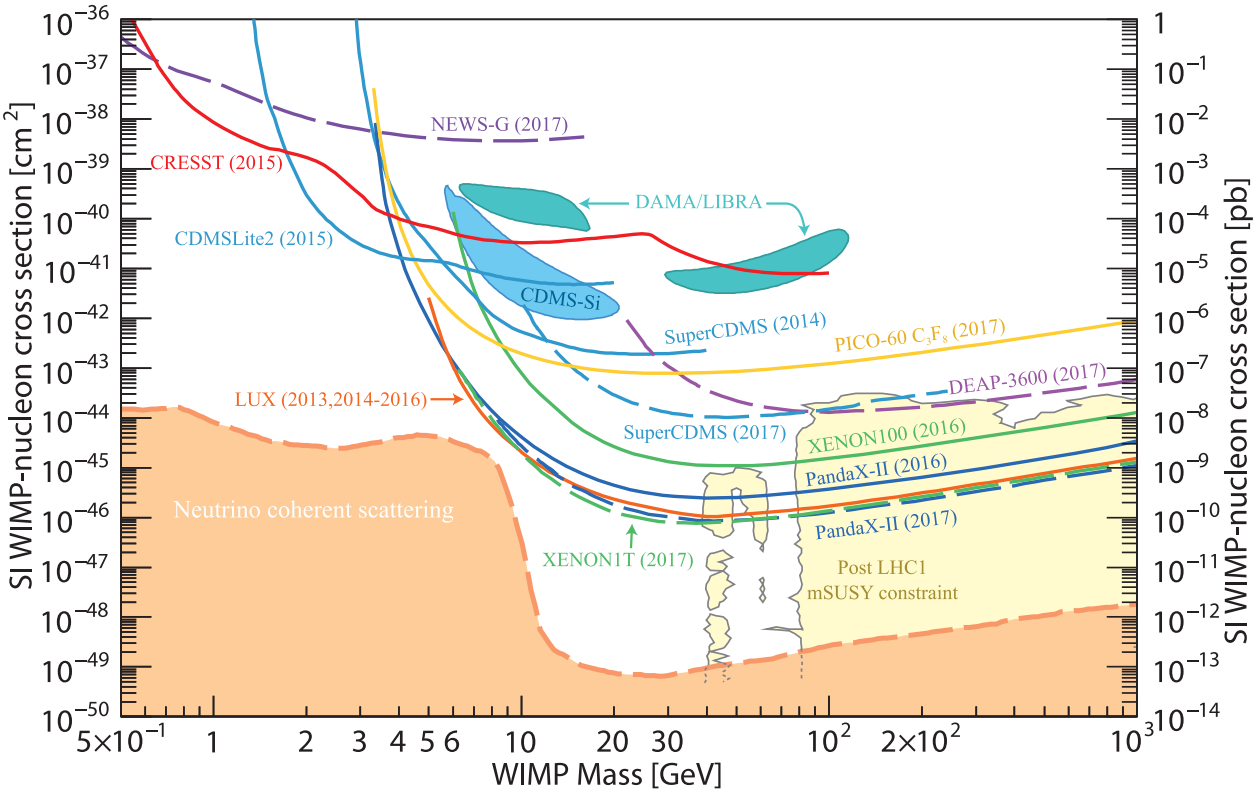

Figure 27.1: WIMP cross sections (normalized to a single nucleon) for spin-independent coupling versus mass. The DAMA/LIBRA [72], and CDMS-Si enclosed areas are regions of interest from possible signal events. References to the experimental results are given in the text. For context, the black contour shows a scan of the parameter space of 4 typical SUSY models, CMSSM, NUHM1, NUHM2, pMSSM10 [73], which integrates constraints set by ATLAS Run 1.

Table 26.1 summarizes the best experimental performances in terms of the upper limit on cross sections for spin independent and spin dependent couplings, at the optimized WIMP mass of each experiment. Also included are some new significant results (using Argon for example).

In summary, the confused situation at low WIMP mass has largely been cleared up (with the notable exception of the DAMA claim). Liquid noble gas detectors have achieved large progress in sensitivity to spin independent coupling WIMPs without seeing any hint of a signal. A lot of progress has also been achieved by the PICO experiment for spin dependent couplings. Many new projects focus on the very low mass range of 0.1-10 GeV. Sensitivities down to $\sigma_{\chi p}$ of 10^{-13} pb, as needed to probe nearly all of the MSSM parameter space [39] at WIMP masses above 10 GeV and to saturate the limit of the irreducible neutrino-induced background [56], will be reached with Ar and/or Xe detectors of multi-ton masses, assuming nearly perfect background discrimination capabilities. For WIMP masses below 10 GeV, this cross section limit is set by the solar neutrinos, inducing an irreducible background at an equivalent cross section around 10^{-9} pb, which is accessible with less massive low threshold detectors [31].

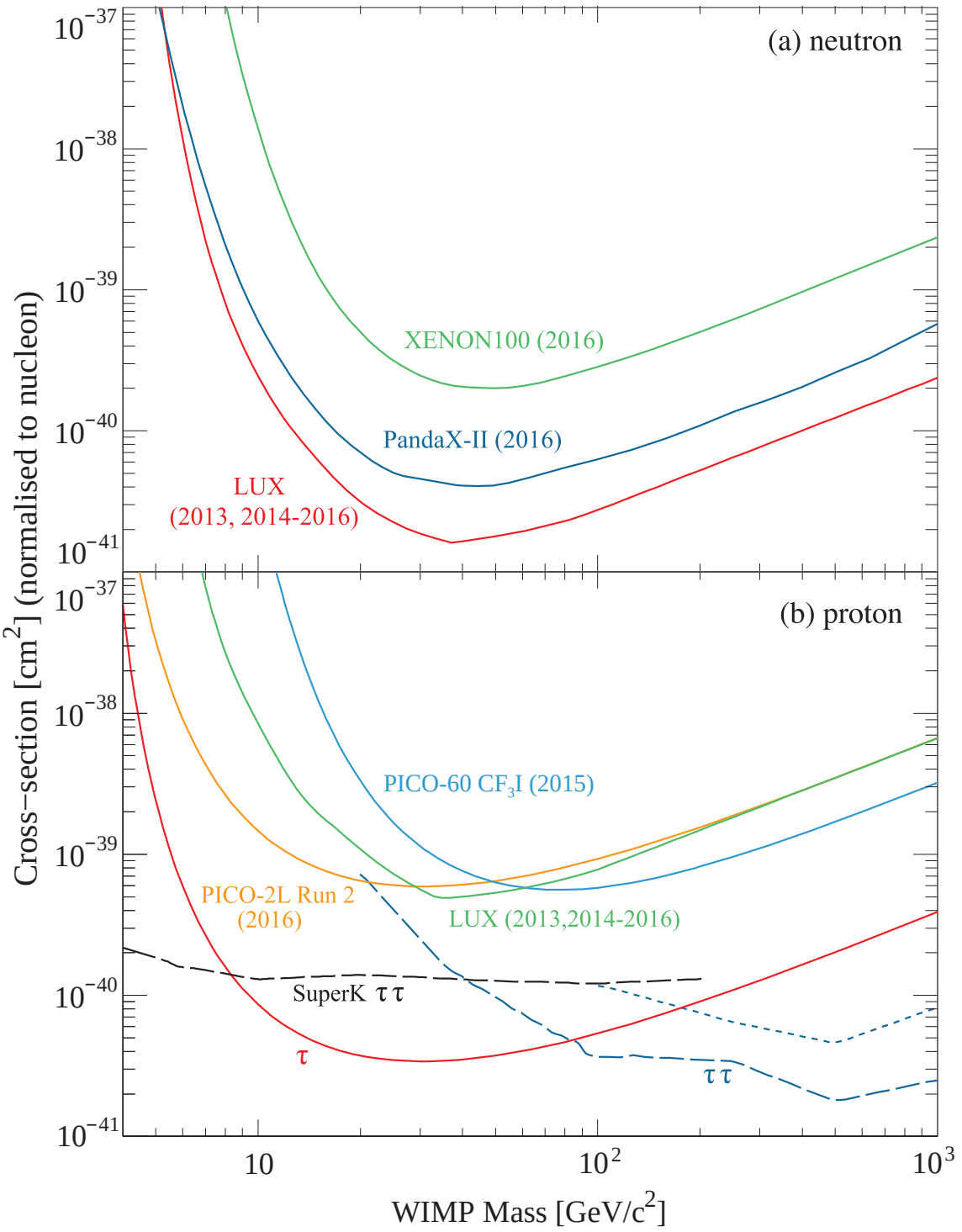

Figure 27.2: WIMP cross sections for spin dependent coupling versus mass. (a) interactions with the neutron; (b) interactions with the proton. References to the experimental results are given in the text. Indirect detection results are from SuperKamiokande (annihilation into $b\bar{b}$ and $\tau^+\tau^-$ channels) together with IceCube (annihilation into W^+W^-); for details see the indirect WIMP searches section below.

Table 27.1: Summary of performances of the best direct detection experiments, for spin independent and spin dependent couplings. For the "low mass" section, in most cases, there is no minimum in the exclusion curve and a best "typical" WIMP mass cross section point has been chosen.

	Target	Fiducial Mass [kg]	Cross section [pb]	WIMP mass [GeV]	Ref.
Spin independent high mass (>10 GeV)					
Xenon1t	Xe	1042	7.7×10^{-11}	35	[49]
PANDAX II	Xe	364	8.6×10^{-11}	40	[53]
LUX	Xe	118	1.1×10^{-10}	50	[50]
SuperCDMS	Ge	12	1.0×10^{-8}	46	[57]
DEAP	Ar	2000	1.2×10^{-8}	100	[55]
Spin independent low mass (<10 GeV)					
LUX	Xe	118	2×10^{-9}	10	[50]
Xenon1t	Xe	1042	2×10^{-9}	10	[49]
PANDAX II	Xe	364	2×10^{-9}	10	[53]
PICO60	C_3F_8 - F	46	2×10^{-7}	10	[67]
SuperCDMS	Ge HV	0.6	3×10^{-5}	3	[58]
CRESST	$CaWO_4$ - O	0.25	1×10^{-2}	1	[63]
NEWS-G	Ne	0.3	6×10^{-2}	1	[66]
Spin dependent p					
PICO60	C_3F_8 - F	54	3.4×10^{-5}	30	[67]
Spin dependent n					
LUX	Xe	118	1.6×10^{-5}	35	[51]

27.2.6. *Status and prospects of indirect WIMP searches* :

WIMPs can annihilate and their annihilation products can be detected; these include neutrinos, gamma rays, positrons, antiprotons, and antinuclei [1]. These methods are complementary to direct detection and might be able to explore higher masses and different coupling scenarios. "Smoking gun" signals for indirect detection are GeV neutrinos coming from the center of the Sun or Earth, and monoenergetic photons from WIMP annihilation in space.

WIMPs can be slowed down, captured, and trapped in celestial objects like the Earth or the Sun, thus enhancing their density and their probability of annihilation. This is a source of muon neutrinos which can interact in the Earth. Upward going muons can then

be detected in large neutrino telescopes such as MACRO, BAKSAN, SuperKamiokande, Baikal, AMANDA, ANTARES, NESTOR, and the large sensitive area IceCube [1]. For standard halo velocity profiles, only the limits from the Sun, which mostly probe spin-dependent couplings, are competitive with direct WIMP search limits.

The best upper limit for low WIMP masses comes from SuperKamiokande [31]. By including events where the muon is produced inside the detector, in addition to the upgoing events used in earlier analyses, they have been able to extend the sensitivity to the few GeV regime. For example, for WIMPs annihilating into $b\bar{b}$ pairs, the resulting upper limit on the spin-dependent scattering cross section on protons is about 1.5 (2.3) fb for $m_\chi = 10$ (50) GeV; for WIMPs annihilating exclusively into $\tau^+\tau^-$ pairs the bounds are about one order of magnitude stronger [74]. These upper bounds are more than two orders of magnitude below the cross sections required to explain the DAMA signal through spin-dependent scattering on protons.

For heavier WIMPs, giving rise to more energetic muons, the best bounds have been derived from IceCube/DeepCore data. These supersede the SuperKamiokande limits for $m_\chi > 40$ (100) GeV if WIMPs annihilate into $\tau^+\tau^-$ ($b\bar{b}$) pairs. For example, the upper bound on the spin-dependent scattering cross section on protons for a 1 TeV WIMP annihilating into W^+W^- is about 0.02 fb; for WIMPs exclusively annihilating into $b\bar{b}$ the bound is about 30 to 100 times weaker [75]. The corresponding upper bounds on spin-independent scattering cross section on protons are about three orders of magnitude stronger; however, they are still at least one order of magnitude weaker than those derived from direct WIMP searches.

WIMP annihilation in the halo can give a continuous spectrum of gamma rays and (at one-loop level) also monoenergetic photon contributions from the $\gamma\gamma$ and γZ channels. These channels also allow to search for WIMPs for which direct detection experiments have little sensitivity, *e.g.*, almost pure higgsinos. The size of this signal depends strongly on the halo model, but is expected to be most prominent near the galactic center. The central region of our galaxy hosts a strong TeV point source discovered [76] by the H.E.S.S. Cherenkov telescope [31]. Moreover, Fermi-LAT [31] data revealed a new extended source of GeV photons near the galactic center above and below the galactic plane, the so-called Fermi bubbles [77], as well as several dozen point sources of GeV photons in the inner kpc of our galaxy [77]. These sources are very likely of (mostly) astrophysical origin. The presence of these unexpected backgrounds makes it more difficult to discover WIMPs in this channel.

Nevertheless analyses of publicly available Fermi-LAT data claimed an excess of events in the few GeV range from an extended region around the center of our galaxy, consistent with several WIMP interpretations [78]. A recent analysis by the Fermi-LAT collaboration [77] indeed found evidence for emission of GeV photons from this region not accounted for by their modeling of astrophysical sources. However, the size, spectrum and morphology of the fitted "excess" depend strongly on the details of the fits. For example, assumptions about the selected region of interest; the template used to model the inverse Compton background; the existence of cosmic ray sources in the inner galaxy; the extension of the "Fermi bubbles" into the galactic center; and about the template for point sources, each can modify the overall flux of the "excess" by a factor $\gtrsim 2$. The

latter two sources of background might each describe the entire "excess" for $E_\gamma \geq 10$ GeV. Note also that most photons detected from directions around the galactic center actually originate from astrophysical foregrounds, not from the central region, and this foreground is not well understood. As a result, a possible signal from WIMP annihilation can contribute at most about 5% of the total photon flux from the direction of the galactic center. Moreover, fitting "WIMP annihilation" templates at different locations around the galactic disk can give even larger "signal-to-background" ratios than that for the galactic center [77]; these "signals" cannot be due to WIMP annihilation, but are due to imperfections of the model used. Fermi-LAT therefore does not claim a signal, but uses these data to constrain a possible contribution from WIMP annihilation. The derived upper bound on the annihilation cross section depends sensitively on the assumed distribution of WIMPs near the galactic center, but is not far worse than the best current bound.

Due to the large astrophysical background near the galactic center, the best bound on WIMPs annihilating into photons in today's universe comes from a combination of Fermi-LAT observations of dwarf galaxies [79]. It excludes WIMPs annihilating either hadronically or into $\tau^+\tau^-$ pairs with the standard cross section needed for thermal relics, if the WIMP mass is below ~ 100 GeV; the main assumption is annihilation from an $S-$wave initial state. Only slightly weaker limits can be derived from detailed analyses of the CMB by the Planck satellite [80]. The CMB bound assumes otherwise standard cosmology, but also holds if WIMPs dominantly annihilate into light charged leptons.

Antiparticles arise as additional WIMP annihilation products in the halo. To date the best measurements of the antiproton flux come from the PAMELA satellite and the AMS-02 experiment [31] on the International Space Station, and cover kinetic energies between 60 MeV and 350 GeV [81]. The result is in fair to good agreement with secondary production and propagation models. These data exclude WIMP models that attempt to explain the "$e^\pm$ excesses" (see below) via annihilation into $W^\pm$ or Z^0 boson pairs; however, largely due to systematic uncertainties they do not significantly constrain conventional WIMP models. The AMS-02 data are sufficiently precise to look for subdominant contributions from WIMP annihilation. Two analyses [82] found statistically quite significant features that could be explained by WIMP annihilation. However, these fits are "suspiciously good". For example, Cuoco *et al.*quote an overall χ^2 of 46 for 163 degrees of freedom. The probability for obtaining this small a χ^2 is below 10^{-20}. The same analysis quotes a χ^2 of 71 for 165 degrees of freedom without a WIMP component. One possible explanation for these anomalously small values of χ^2 are correlations between the experimental errors that have not been accounted for.

The best measurements of the positron (and electron) flux at energies of tens to hundreds GeV also come from AMS02 [83] and PAMELA [84], showing a rather marked rise of the positron fraction between 10 and 200 GeV; the AMS02 data are compatible with a flattening of the positron fraction at the highest energies. While the observed positron spectrum falls within the one order of magnitude span (largely due to differences in the propagation model used) of fluxes predicted by secondary production models [85], the increase of the positron fraction is difficult to reconcile with the rather hard electron spectrum measured by PAMELA [86], if all positrons were due to secondary interactions

of cosmic ray particles. Measurements of the total electron+positron energy spectrum by ATIC [87], Fermi-LAT [88] and H.E.S.S. [89] between 100 and 2000 GeV also exceed the predicted purely secondary spectrum, but with very large dispersion of the magnitude of these excesses. These observations can in principle be explained through WIMP annihilation. However, this requires cross sections well above that indicated by Eq. (27.6) for a thermal WIMP. This tension can be resolved only in somewhat baroque WIMP models. Most of these models have by now been excluded by the stringent bounds from Fermi-LAT and from analyses of the CMB on the flux of high energy photons due to WIMP annihilation. This is true also for models trying to explain the leptonic excesses through the decay of WIMPs with lifetime of the order of 10^{26} s. In contrast, viable astrophysical explanations of these excesses introducing new primary sources of electrons and positrons, e.g. pulsars [90] or a nearby supernova that exploded about two million years ago [91], have been suggested. On the other hand, the high quality of the AMS02 data on the positron fraction, which does not show any marked features, allows one to impose stringent bounds on WIMPs with mass below 300 GeV annihilating directly into leptons [92]. However, for energies between 100 GeV and 1 TeV the latest Fermi-LAT result for the summed electron+positron flux is significantly above that from AMS-02.

Last but not least, an antideuteron signal [1], as potentially observable by AMS02 or PAMELA, could constitute a signal for WIMP annihilation in the halo.

An interesting comparison of respective sensitivities to MSSM parameter space of future direct and various indirect searches has been performed with the DARKSUSY tool [93]. A web-based up-to-date collection of results from direct WIMP searches, theoretical predictions, and sensitivities of future experiments can be found in [71]. Also, the web page [94] allows to make predictions for WIMP signals in various experiments, within a variety of SUSY models and to extract limits from simply parameterized data. Integrated analysis of all data from direct and indirect WIMP detection, and also from LHC experiments should converge to a comprehensive approach, required to fully unravel the mysteries of dark matter.

References:

1. For details, recent reviews and many more references about particle dark matter, see G. Bertone, *Particle Dark Matter* (Cambridge University Press, 2010).
2. For a brief but delightful history of DM, see V. Trimble, in *Proceedings of the First International Symposium on Sources of Dark Matter in the Universe*, Bel Air, California, 1994, published by World Scientific, Singapore (ed. D.B. Cline). See also the recent review G. Bertone, D. Hooper, and J. Silk, Phys. Reports **405**, 279 (2005).
3. E.W. Kolb and M.E. Turner, *The Early Universe*, Addison-Wesley (1990).
4. M. Milgrom, Can. J. Phys. **93**, 107 (2015), and references therein.
5. See e.g. L. Bernard and L. Blanchet, Phys. Rev. D 91,103536(2015).
6. See the section on *Experimental Tests of Gravitational Theory* in this *Review*.
7. See *Cosmological Parameters* in this *Review*.
8. B. Paczynski, Astrophys. J. **304**, 1 (1986);
   K. Griest, Astrophys. J. **366**, 412 (1991).
9. F. De Paolis *et al.*, Phys. Rev. Lett. **74**, 14 (1995).

10. R. Catena and P. Ullio, JCAP **1008**, 004 (2010).
11. M. Pato *et al.*, Phys. Rev. **D82**, 023531 (2010).
12. N. Bernal *et al.*, JCAP **1409**, 004 (2014).
13. J. Bovy and S. Tremaine, Astrophys. J. **756**, 89 (2012).
14. K. Kohri, D.H. Lyth, and A. Melchiorri, JCAP **0804**, 038 (2008).
15. B. Carr *et al.*, Phys. Rev. **D96**, 023514 (2017).
16. See *Axions and Other Very Light Bosons* in this *Review*.
17. A. Kusenko, Phys. Reports **481**, 1 (2009).
18. For a general introduction to SUSY, see the section devoted in this *Review of Particle Physics*. For a review of SUSY Dark Matter, see G. Jungman, M. Kamionkowski, and K. Griest, Phys. Reports **267**, 195 (1996).
19. See *Searches for WIMPs and Other Particles* in this *Review*.
20. T. Moroi and L. Randall, Nucl. Phys. **B570**, 455 (2000).
21. R. Allahverdi and M. Drees, Phys. Rev. Lett. **89**, 091302 (2002).
22. M. Fujii and T. Yanagida, Phys. Lett. **B542**, 80 (2002).
23. J. Hisano, K. Kohri, and M.M. Nojiri, Phys. Lett. **B505**, 169 (2001).
24. D.E. Kaplan, M.A. Luty, and K.M. Zurek, Phys. Rev. **D79**, 115016 (2009).
25. G. Belanger *et al.*, Phys. Lett. **B726**, 773 (2013).
26. J. Kozaczuk and S. Profumo, Phys. Rev. **D89**, 095012 (2014).
27. N. Arkani-Hamed *et al.*, Phys. Rev. **D79**, 015014 (2009).
28. A. Soffner, `arXiv:1507.02330`, and references therein;
    BaBar Collab., J.P. Lees *et al.*, `arXiv:1702.03327`.
29. Y. Hochberg *et al.*, Phys. Rev. Lett. **113**, 171301 (2014).
30. MACHO Collab., C. Alcock *et al.*, Astrophys. J. **542**, 257 (2000);
    EROS-2 Collab., P. Tisserand *et al.*, Astron. & Astrophys. **469**, 387 (2007);
    OGLE Collab., L. Wyrzykowski *et al.*, Mon. Not. R. Astron. Soc **416**, 2949 (2011).
31. A very useful collection of web links to the homepages of Dark Matter related conferences, and of experiments searching for WIMP Dark Matter, is the "Dark Matter Portal" at `http://lpsc.in2p3.fr/mayet/dm.php`. See also the TAUP and IDM conference series sites : `http://www.taup-conference.to.infn.it` and `http://kicp-workshops.uchicago.edu/IDM2012/overview.php`.
32. S.J. Asztalos *et al.*, Phys. Rev. **D69**, 011101 (2004);
    S.J. Asztalos *et al.*, Phys. Rev. Lett. **104**, 041301 (2010).
33. L.D. Duffy *et al.*, Phys. Rev. **D74**, 012006 (2006);
    J. Hoskins *et al.*, Phys. Rev. **D84**, 121302 (2011).
34. A. Ringwald, t arXiv:1612.08933.
35. E. Bulbul *et al.*, Astrophys. J. **789**, 13 (2014);
    O. Ruchayskiy *et al.*, Mon. Not. R. Astron. Soc **460**, 1390 (2016);
    J. Franse *et al.*, Astrophys. J. **829**, 124 (2016).
36. O. Urban *et al.*, Mon. Not. R. Astron. Soc **451**, 2447 (2015);
    F.A. Aharonian *et al.*, Astrophys. J. **837**, L15 (2017).
37. T.E. Jeltema and S. Profumo, Mon. Not. R. Astron. Soc **450**, 2143 (2015) and references therein.
38. M.C. Smith *et al.*, Mon. Not. R. Astron. Soc **379**, 755 (2007).

39. J. Ellis *et al.*, Phys. Rev. **D77**, 065026 (2008).
40. C.E. Aalseth *et al.*, Phys. Rev. Lett. **106**, 131301 (2011).
41. XENON100 Collab., E. Aprile *et al.*, Phys. Rev. Lett. **109**, 181301 (2012).
42. CDEX Collab., W. Zhao *et al.*, Phys. Rev. **D93**, 092003 (2016).
43. DAMA Collab., R. Bernabei *et al.*, Phys. of Part. and Nucl. **46**, 2 (2015), Phys. of Part. and Nucl. **46**, 138 (2015).
44. M. Fairbairn and T. Schwetz, JCAP **0901**, 037 (2009).
45. C. Kelso, AIP Conf. Proc. **1743**, 050007 (2016).
46. S.C. Kim *et al.*, Phys. Rev. Lett. **108**, 181301 (2012).
47. K. Kim *et al.*, IEEE Trans. **NS63**, 534 (2016).
48. DM Ice Collab., E. Barbosa de Souza *et al.*, Phys. Rev. **D95**, 032006 (2017).
49. XENON Collab., E. Aprile *et al.*, `arXiv:1705.06655`, Phys. Rev. **D94**, 122001 (2016).
50. LUX Collab., D.S. Akerib *et al.*, Phys. Rev. Lett. **118**, 021303 (2017).
51. LUX Collab., D.S. Akerib *et al.*, Phys. Rev. Lett. **118**, 251302 (2017).
52. PandaX Collab., A. Tan *et al.*, Phys. Rev. Lett. **117**, 121303 (2016).
53. PandaX-II Collab., X. Cui *et al.*, `arXiv:1708.06917`.
54. DarkSide Collab., P. Agnes *et al.*, Phys. Rev. **D93**, 081101 (2016).
55. DEAP Collab., P.-A. Amaudruz *et al.*, `arXiv:1707.08042`.
56. J. Billard, L. Strigari, E. Figueroa-Feliciano, Phys. Rev. **D89**, 023524 (2014).
57. SuperCDMS Collab., R. Agnese *et al.*, `arXiv:1708.08869`, Phys. Rev. Lett. **112**, 241302 (2014), Phys. Rev. **D92**, 072003 (2015).
58. SuperCDMS Collab., R. Agnese *et al.*, Phys. Rev. Lett. **116**, 071301 (2016).
59. SuperCDMS Collab., R. Agnese *et al.*, Phys. Rev. **D95**, 082002 (2017).
60. Edelweiss Collab., L. Hehn *et al.*, Eur. Phys. J. **C76**, 548 (2016).
61. Edelweiss Collab., Q. Arnaud *et al.*, `arXiv:1707.04308`.
62. COHERENT Collab., D. Akimov *et al.*., `arXiv:1708.04255`, published in Science (Aug. 2017).
63. CRESST Collab., G. Angloher *et al.*, Eur. Phys. J. **C76**, 25 (2016).
64. CRESST Collab., G. Angloher *et al.*, `arXiv:1707.06749`.
65. DAMIC Collab., A. Aguilar-Arevalo *et al.*, Phys. Rev. **D94**, 082006 (2016).
66. NEWS-G Collab., Q. Arnaud *et al.*, `arXiv:1706.04934`.
67. PICO Collab., C. Amole *et al.*, Phys. Rev. Lett. **118**, 251301 (2017).
68. DRIFT Collab., J.B.R. Battat *et al.*, Astropart. Phys. **91**, 65 (2017).
69. NEWSdm Collab., N. di Marco *et al.*, J. Phys. Conf. Ser. **718**, 042018 (2016).
70. Community paper `arXiv:1707.04591`, proceedings of U.S. Cosmic Visions: New Ideas in Dark Matter, `https://indico.fnal.gov/event/13702/`.
71. DMTOOLS site : `http://dmtools.brown.edu:8080/`.
72. C. Savage *et al.*., JCAP **0904**, 010 (2009).
73. E.A. Bagnaschi *et al.*, Eur. Phys. J. **C75**, 500 (2015).
74. SuperKamiokande Collab., K. Choi *et al.*, Phys. Rev. Lett. **114**, 141301 (2015).
75. IceCube Collab., M.G. Aartsen *et al.*, Eur. Phys. J. **C77**, 146 (2017).
76. H.E.S.S. Collab., F. Aharonian *et al.*, Astron. & Astrophys. **503**, 817 (2009); H.E.S.S. Collab., F. Acero *et al.*, Mon. Not. R. Astron. Soc **402**, 1877 (2010).

77. Fermi-LAT Collab., M. Ackermann *et al.*, Astrophys. J. **840**, 43 (2017).
78. D. Hooper and L. Goodenough, Phys. Lett. **B697**, 412 (2011);
T. Daylan *et al.*, Phys. Dark Univ. **12**, 1 (2016).
79. Fermi-LAT Collab., M. Ackermann *et al.*, Phys. Rev. Lett. **115**, 231301 (2015).
80. G. Steigman, Phys. Rev. **D91**, 083538 (2015).
81. PAMELA Collab., O. Adriani *et al.*, Phys. Rev. Lett. **105**, 121101 (2010);
AMS-02 Collab., M. Aguilar *et al.*, Phys. Rev. Lett. **117**, 091103 (2016).
82. M.Y. Cui, Q. Yuan, Y.L. Sming Tsai and Y.Z. Fan, Phys. Rev. Lett. **118**, 191101 (2017);
A. Cuoco, M. Krämer and M. Korsmeier, Phys. Rev. Lett. **118**, 191102 (2017).
83. AMS02 Collab., M. Aguilar *et al.*, Phys. Rev. Lett. **113**, 121101 (2014) and Phys. Rev. Lett. **113**, 121102 (2014).
84. PAMELA Collab., O. Adriani *et al.*, Phys. Rev. Lett. **111**, 081102 (2013).
85. T. Delahaye *et al.*, Astron. & Astrophys. **501**, 821 (2009).
86. PAMELA Collab., O. Adriani *et al.*, Phys. Rev. Lett. **106**, 201101 (2011).
87. ATIC Collab., J. Chang *et al.*, Nature **456**, 362 (2008).
88. Fermi-LAT Collab., S. Abdollahi *et al.*, Phys. Rev. **D95**, 082007 (2017).
89. H.E.S.S. Collab., F. Aharonian *et al.*, Astron. & Astrophys. **508**, 561 (2009).
90. M. Cirelli, Pramana **79**, 1021 (2012);
S. Profumo, Central Eur. J. Phys. **10**, 1 (2011).
91. M. Kachelriess, A. Neronov, D.V. Semikoz, Phys. Rev. Lett. **115**, 181103 (2015).
92. L. Bergstrom *et al.*, Phys. Rev. Lett. **111**, 171101 (2013).
93. DARKSUSY site: `http://www.physto.se/~edsjo/darksusy/`.
94. ILIAS web page: `http://pisrv0.pit.physik.uni-tuebingen.de/darkmatter/`.